# FLIGHT SOUND OF AN INSECT WING: APPLICATION OF METAMATERIAL CONCEPTS TO BIOINSPIRED FLAPPING WINGS

Mostafa Ranjbar Cranfield University, Centre for Energy Engineering, UNITED KINGDOM
M. Cihat Yilmaz Ankara Yildirim Beyazit University, Mechanical Eng. Department, TURKIYE

## 1 INTRODUCTION

Architecture is critical for fundamental functions and bio-physical characteristics of biological materials. For instance, the shape and arrangements of material building blocks at various levels, from nano- to macroscale, deliver superior mechanical properties, such as extreme hardness of teeth, ultra-high specific stiffness of wood (comparable to steel), and extraordinary strength of nacre[1,2]. These and other examples inspired researchers to develop advanced technological materials with functionalities driven by their structure rather than constituents – metamaterials[3]. As a result, there emerged ultra-lightweight metallic materials[4], extremely stiff[5,] and fluid-type[6] cellular materials, strong and recoverable nano-structured lattices[7]. In acoustics and wave dynamics, bio-inspired designs have opened a way to achieve broadband[8] and tunable[9] manipulation of structural and acoustic waves.

Yet, the functionality of architecture goes even further by allowing biomaterials to act as mechanisms that enable adaptation to changing environmental conditions and various load combinations. A prominent example is insect wings. These are lightweight structures (of a mass lower than 2% of an insect's total weight) that have a high load-bearing capacity, can cope with attacking aerodynamic forces[10,] and accelerate the surrounding air to enable flight[11]. Multiple studies have shown that these abilities originate exclusively from the structure and distribution of a building material[10,12,13,14,15,16].

The advances in finite-element techniques enabled to reproduction of complex aerodynamic conditions of different types of flight and to investigate the influence of the material architecture on mechanical and aerodynamic characteristics of insect wings[17,18,19,20]. For example, it was found that intricate venation patterns of the dragonfly and hoverfly wings help to minimize the mass of the wing and to ensure the balance between flexibility and rigidity[21]. The latter delivers a required lift force[11] and reduces peak driving forces and power consumption[18,22]. The three-dimensional configuration of a wing is responsible for its stability and appropriate operation[10]. Besides, it appeared that wingbeat frequency is not linked to the structural resonant frequency of the wing[14]. Yet, the existing studies pay little, if not at all, attention to the vibro-acoustics of a wing, i.e., to the sound generation process during flight[23]. This aspect is relevant in light of applications of bio-inspired concepts to the design of artificial wings for micro-robotic devices[24,25].

This work aims at filling in this gap and presents an in-depth analysis of noise radiation conditions and their dependence on the mechanical and material characteristics of a wing. We consider the flapping flight of an artificial flexible wing with an architecture of a dragonfly wing. The aerodynamics of flapping flexible wings is especially promising for flying robots due to their wind tolerance, efficient lift power, and the possibility to stop during flight[24]. Our goal here is to understand how the material and morphological parameters of a wing can be manipulated to minimize the radiated sound by simultaneously preserving the attractive features of flexible wings. In other words, we want to verify whether the metamaterial concepts implying tailored design of individual material elements can be used to modify the vibroacoustic characteristics of bio-inspired wings.

The remaining text is structured as follows. First, we introduce a model of a flapping artificial wing and our analysis approach (Section 2). Then, we study the structural dynamic and vibroacoustic characteristics of the wing and estimate the influence of mechanical and material properties on the radiated sound (Section 3). Next, we demonstrate how local variations of the mechanical and material properties can be used to control the generated noise which opens a promising way towards the

design of “quiet” wings (Section 4). We finalize the work with concluding remarks and by speculating on possible future research directions.

# 2 MODEL AND ANALYSIS

## 2.1 Model of a Wing

Our wing model reproduces a real dragonfly wing, M. septendecim (Figure 1, left). The model is 40 mm long, 15.25 mm breed and has a surface area of 414 $mm^2$, that is very close to original dimensions of the wing[26].

The shape and the structure of the wing are important as governing its structural, aerodynamic and acoustic characteristics[10,18,27]. Therefore, we accurately reproduced the in-plane configuration of veins and membranes, while the out-of-plane structure can be simplified by assuming a uniform varying thickness from 0.45 mm to 0.1 mm (Figure 1, right)[18,28]. The top of the wing is thus naturally reinforced by its three-dimensional structure.

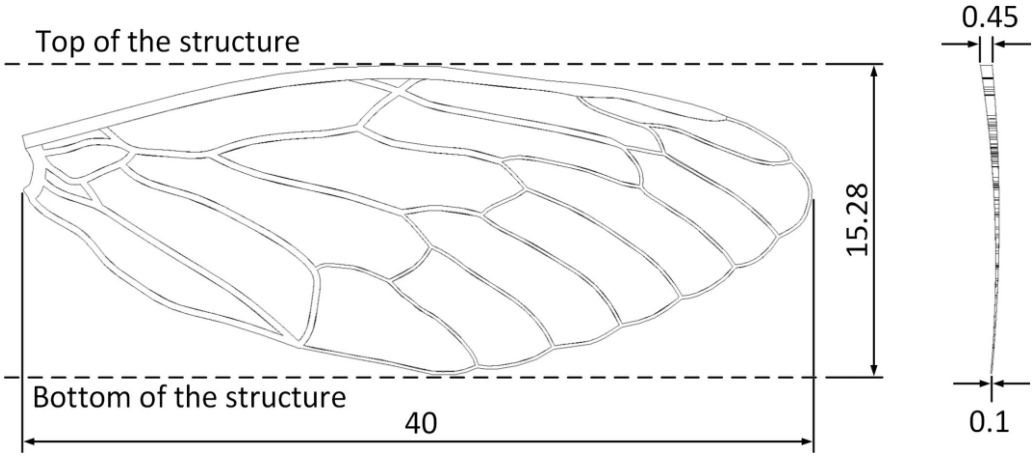


**Figure 1** Geometric model of an insect wing. The indicated dimensions are in mm.

We consider a flapping flight that can be described by a simple load case ignoring the angle of attack[10,12]. The body of an insect can be omitted from consideration as it has a negligible effect on the wing dynamics and airflow[18]. These simplifications allow us to identify the role of individual structural components avoiding multi-scale modeling, despite the complex venation pattern.

To imitate flapping, we assign a harmonic loading $A_0 \sin(2\pi ft)$ perpendicular to the wing surface from below to induce rotations along the dorsal-ventral direction (the x-axis in Figure A1a). The rotations occur at close to a realistic flapping frequency f =100 Hz and amplitude $A_0 = 70^o$ within 0.15 sec. These values correspond to an angular velocity of 4.884 rad/s and a tangential velocity of 0.195 m/s at the top of the wing. The nodes at the base are fixed to exclude translational motions. The initial conditions imply zero displacement and zero velocity at all nodes.

The real dragonfly wing consists of chitin with a mass density of 1200 $kg/m^3$, Poisson’s ratio of 0.25, and Young’s modulus of about 6 GPa[10,12,29]. It is reasonable to assume isotropic mechanical behavior and uniform distribution of the mass within the wing[18].

To investigate the relationship between the material and mechanical properties and sound radiation conditions, we consider a model of an imaginary wing with varying Young’s modulus and mass density values, as described below. Poisson’s ratio has a small effect on the wing dynamics and is fixed.

## 2.2 Modelling Approach

The flapping flight conditions are reproduced numerically by means of the finite-element method in ANSYS (Ansys® Academic Research Mechanical, Release 19.3). A full modelling cycle includes (1) a modal analysis to study admissible structural deformations of the wing; (2) a harmonic analysis to estimate excitation amplitudes; (3) a transient analysis to model strong interactions between induced deformations of the wing and the surrounding air. The transient analysis based on fluid-structure interactions (FSI) implies the use of a common moving mesh for the air and the wing[18].

The total simulation time of the full cycle is about 27 minutes at a desktop computer (7 cores, 3.40 GHz, 16 GB RAM). In particular, the modal analysis for the model with Tet10 finite elements runs for about 1 min. The harmonic analysis includes a harmonic response (about 11 min) and a harmonic acoustics (about 3 min) for the same mesh. Finally, the transient analysis is composed of a transient structural analysis (Tet10, Hex20 and Wed15 elements with the average simulation time of about 1 min), a transient fluent analysis (Tet4 elements; about 1 min), and a system coupling (about 10 min).

The finite-element model is represented by the wing model meshed by thin-shell elements and a surrounding cubic box of 300 mm length filled with air. This size of the box is sufficient to exclude the influence of boundary conditions at the box edges[18]. The mesh sensitivity analysis showed that the results obtained for normal (29844 elements) and fine (95204 elements) meshes differ by less than 1%. Hence, the normal mesh was used for the simulations (Figure A1b).

# 3 STRUCTURAL DYNAMICS AND SOUND GENERATION BY AN ARTIFICIAL WING

The modal analysis delivers structural eigenfrequencies and eigenmodes essential tointerpret the results of transient simulations.

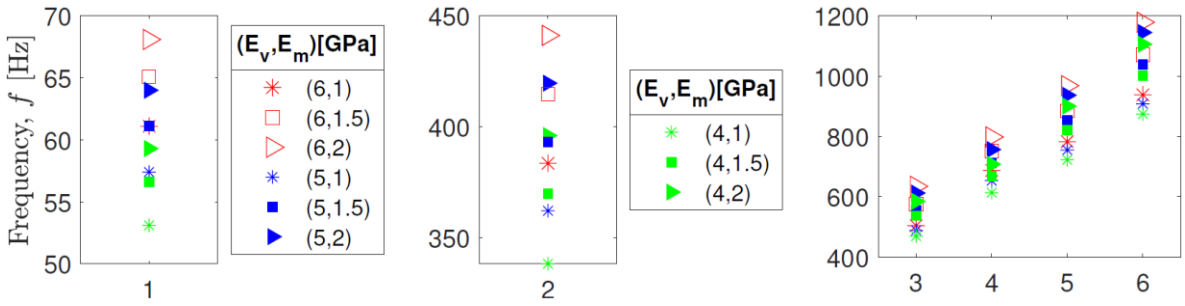


**Figure 2** The effect of the Young's moduli variations for the veins $E_v$ and membranes, $E_m$ on the first six eigenfrequencies of the wing.

We consider the first six eigenfrequencies and assume $E_v$ to be equal to 6 GPa,5 GPa or 4 GPa. In each of these cases, $E_m$ equals to either 2 GPa, 1.5 GPa, or 1 GPa. The eigenfrequency values are given in Figure 2. As can be seen, they are below 1200 Hz that will be considered as an upper liming frequency in the transient analysis. The first eigenfrequency varies between 53 Hz and 68 Hz for the analyzed values of $E_v$ and $E_m$. Expectedly, a stiffer wing, i.e., with larger values of $E_v$ and $E_m$, has larger eigenfrequencies.

The eigenmodes appear to be insensitive to the considered variations of $E_v$, $E_m$. For example, Figure 3 shows six eigenmodes for $E_v$ = 6 GPa and $E_m$ = 1 GPa, which arevery similar to the modes for the other values of $E_v$ and $E_m$ (not shown). The color indicates the deformation distribution from zero (dark blue) to a maximum value (red). The first two and the fourth mode shapes describe bending motions, while the otherthree correspond to flexural modes.

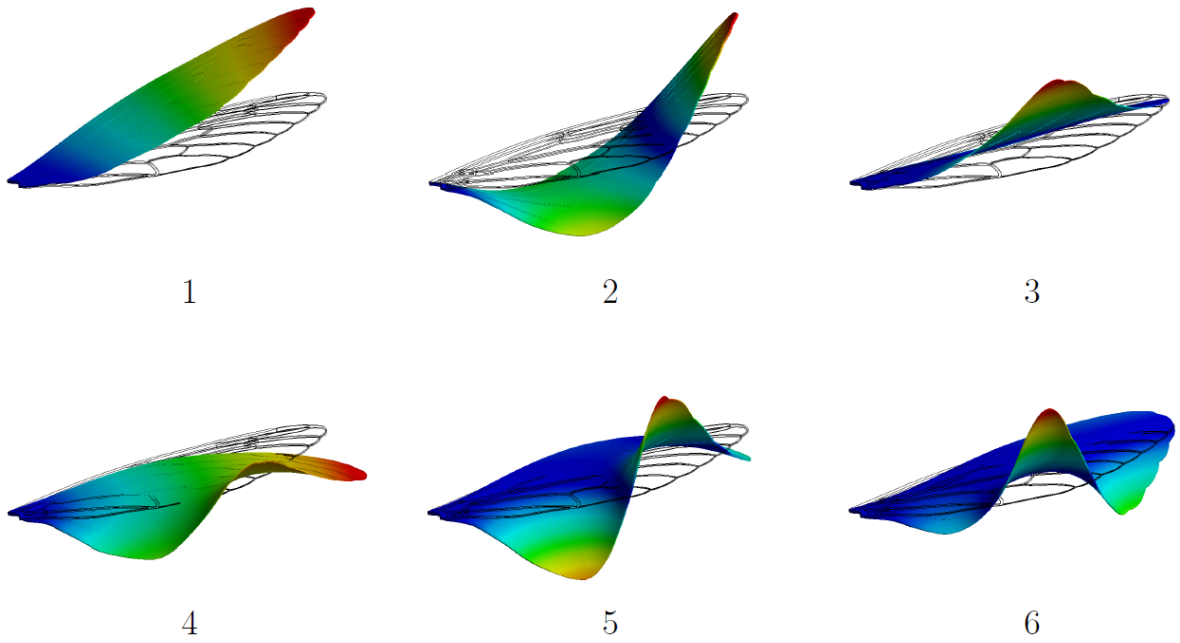


**Figure 3** The mode shapes of the first six eigenmodes of the wing.

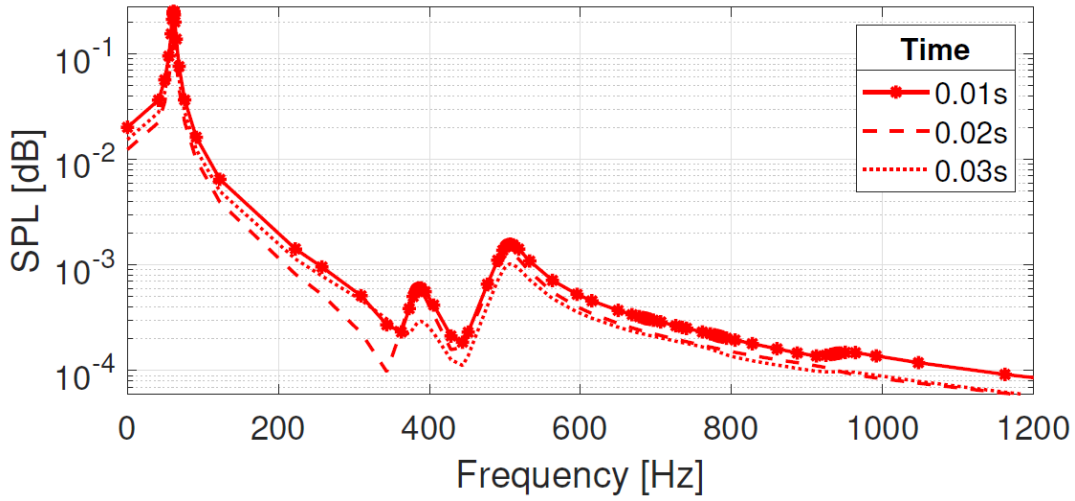


**Figure 4** Effect of material property variations on the FRF of the bioinspired model for $E_v$ = 6 GPa, $E_m$ = 1 GPa

We proceed by analyzing the frequency response function (FRF) that indicates the efficiency of the mode excitation under the applied loading. Figure 4 shows the modal amplitudes at the beginning of a flapping cycle for $E_v$ = 6 GPa, $E_m$ = 1 GPa. One can see that only the first three eigenmodes are efficiently excited. The first mode has the strongest with the amplitude exceeding that of the other modes by at least two orders. This occurs due to a match between the modal shape and the applied loading, but also due to a low damping for this mode, as discussed below. Note that the excitation efficiency is preserved in time.

The trends of the FRF curves for the other values of the Young's moduli exhibit only small differences with respect to those shown in Figure 4, and thus, are not presented here. We can conclude that the considered variations of $E_v$ and $E_m$ do not influence the efficiency of the mode excitation. Hence, one can expect the strongest contribution of the first eigenmode into the noise generation process during the flight.

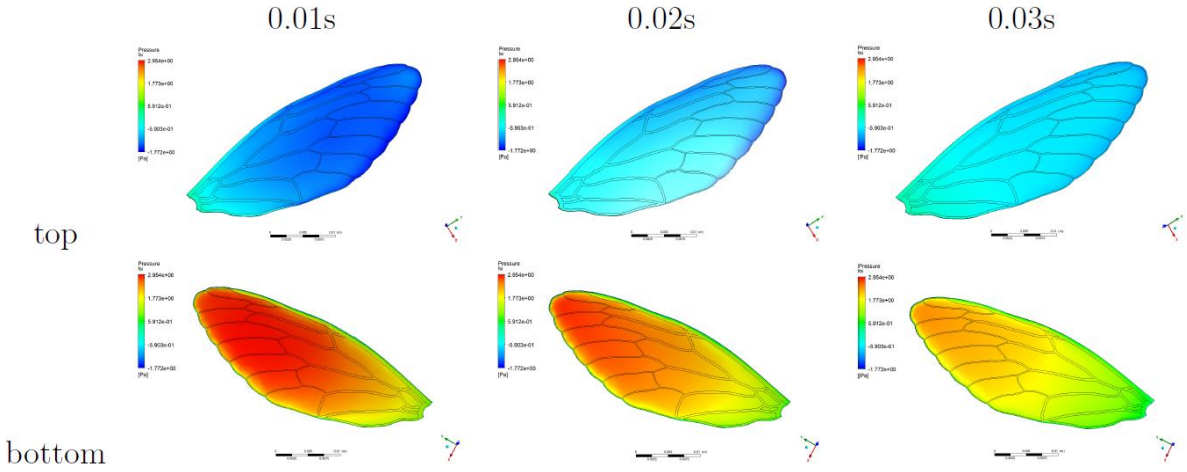


**Figure 5** Pressure areas on the bioinspired model $E_v$ = 6GPa, $E_m$ = 1 GPa

Further, we investigate the pressure distribution near the wing surfaces. This can be done by coupling structural motions calculated by the energy method[30] with the fluent analysis results by means of the FSI. The FSI is introduced by a pressure-velocity coupling and using a transient pressure-based solver[24]. Since our approach does not allow controlling aerodynamic forces, we apply a damping factor to stabilize the model[12]. The calculations show that a constant value of 0.004 for the damping factor, corresponding to the Mach number of 0.000569, is sufficient to reduce high-frequency vibrations and agrees well with the data reported elsewhere[31].

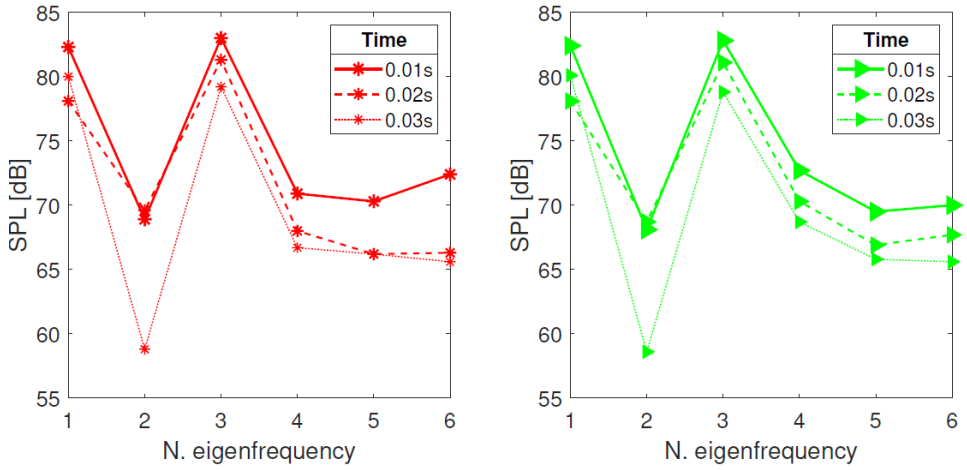


**Figure 6** Sound pressure level (SPL) at each eigenfrequency at in different moments of time: $E_v$ = 6 GPa, $E_m$ = 1 GPa (left) and $E_v$ = 4 GPa, $E_m$ = 2 GPa (right)

The pressure was estimated by extracting drag and lift forces in different moments of time. The calculations reveal that the maximum pressure is achieved at the beginning of a flapping cycle. For example, Figure 5 shows the pressure at the top and bottom surfaces of the wing at 0.01, 0.02 and 0.03 s after the start of a cycle. The top (unloaded) surface, obviously, has a lower pressure magnitude than the bottom surface. The pressure at the bottom surface is concentrated mainly at the tip which agrees with the measurement results for a real insect wing[10,18]. At the top surface, the pressure is larger near the base of the wing, where the real insect wing is reinforced by thicker veins. The results in Figure 5 are for $E_v$ = 6 GPa and $E_m$ = 1 GPa. Can we expect different pressure distributions if the mechanical properties are changed? The simulations show that by increasing the stiffness of membranes, the overall pressure can be slightly reduced but is distributed over a wider area (see Figures A2 and A3 for details).

An intrinsic product of the oscillating pressure is sound. To get insight into the sound generation process, we estimated the maximum sound pressure level (SPL) around the wing. Figure 6 shows representative time-dependencies of the SPL at the eigenmodes for the two specified sets of $E_v$, $E_m$. For the other Young's moduli, these dependencies are very similar to those in Figure 6 and are not shown. This means that the radiatednoise is almost independent of the stiffness of the veins and membranes.

The first mode, indeed, generates strong sound monotonically decreasing in time. Surprisingly, the third eigenmode radiates the same amount of sound. We remind you that the third mode is the lowest flexural mode (Figure 3). Hence, the total noise is produced by two fundamental modes equally contributing to this process, despite large differences in their excitation amplitudes (Figure 4 left). The second and higher modes produce much less sound, at least by 10 dB. This sound also decreases in time, sometimes non- monotonically that can be explained by changes in the areas of the maximum pressure distribution over the wing surface (Figure 5).

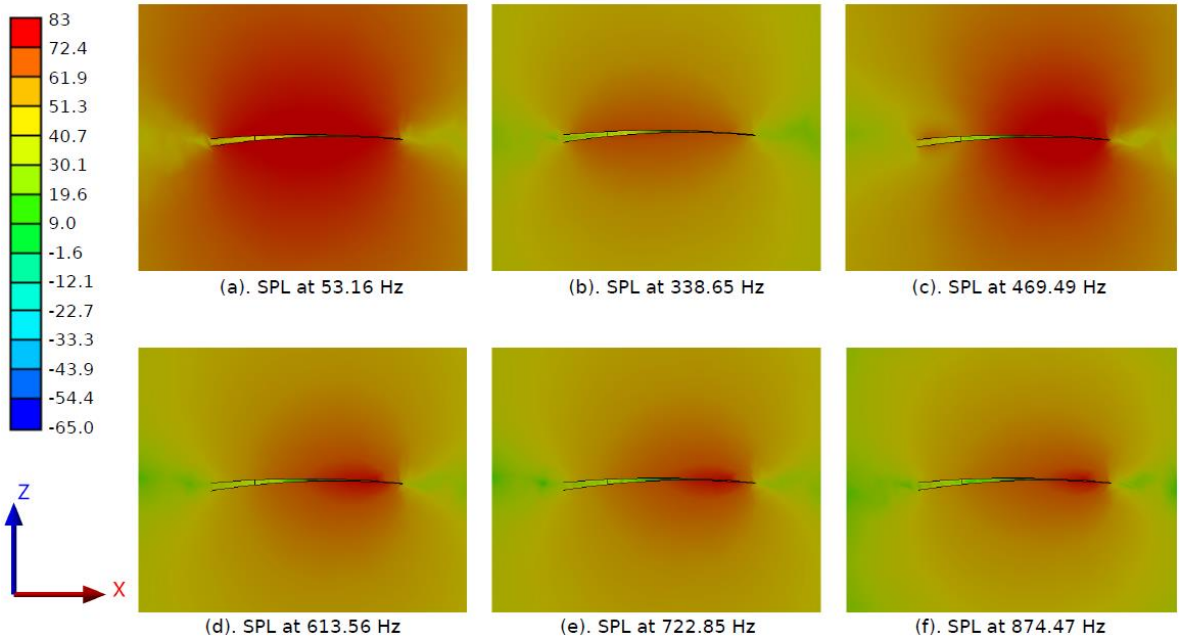


**Figure 7** SPL distribution in (dB) for each modal frequency of the bioinspired model, $E_v$ = 4 GPa, $E_m$ = 1 GPa, after 0.01 second from the start of the flapping cycle

The sound distribution in the air around the wing is shown in Figure 7 for each eigenmode at the beginning of a flapping cycle. It is clearly non-uniform and decreases with the distance from the wing. To estimate preferred propagation directions, we consider three normal cross-sections A, B and C in the chord direction with eight measurement points located at a circle of radius 15 mm and a 45◦ angle between neighboring points (Figure 8). As these points, the maximum SPL values are calculated as shown in Figure 9 for two representative cases.

The results reveal that the strongest sound is radiated perpendicular to the wing plane, regardless of the distance from the base. Note that the further from the center of the wing, the lower the SPL. Since the base contains more veins compared to the tip, we conclude that a stiffer part of the wing generates more noise. However, the overall sound level seems to be independent of the variation of $E_v$ and $E_m$, as follows from the comparison of Figures 9a and 9b. The sound distribution above and below the wing is not fully symmetric that can be explained by the non-symmetric pressure distribution at the flexural mode (Figure 3).

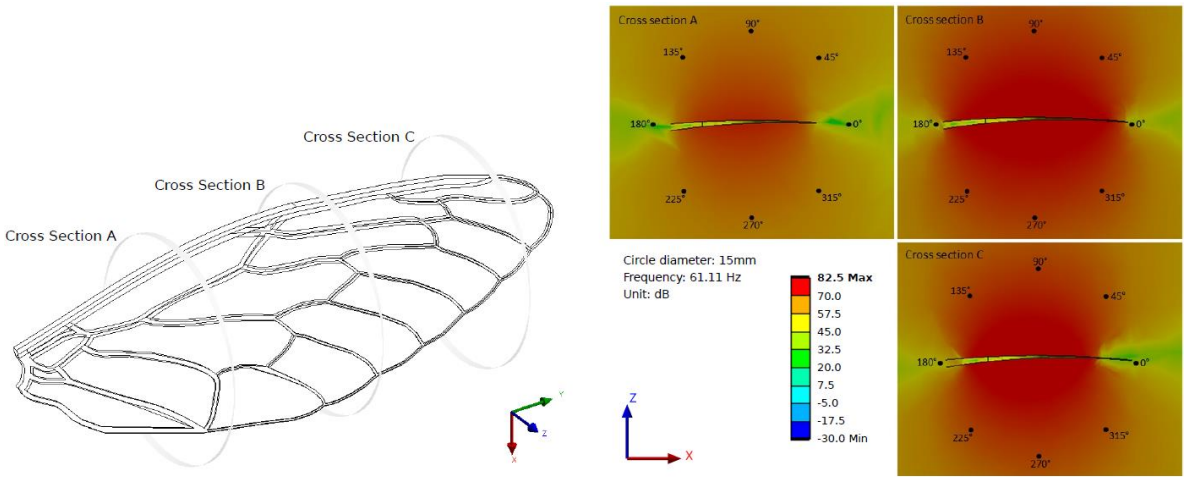


**Figure 8** Directional noise: (left) Positions of the A, B, and C cross-sections at 10 mm, 20 mm, and 30 mm distance from the base of the wing. (right) The analysis points at the radius of 15 mm in various angles around the model in each cross-section

We remind that in this study the noise is generated solely by structural motions and not by the surface viscosity effects, as the surface of the wing is assumed to be smooth. The surface of the real dragonfly wing is not smooth; thus, the related viscosity effects can substantially influence the sound radiation conditions[27].


**Figure 9** SPL in each cross-section of A, B and C around the wing in various angles

Finally, we evaluated the effects of the material density variations on the structuraldynamics and the noise radiation of the wing. We considered a "soft" wing with $E_v = E_m = 2$ GPa and used the same value of $\rho$ for the veins and membranes. As can be expected, a heavier wing has lower eigenfrequencies (Figure 10) in opposite to the effect of increasing stiffness (Figure 2). The harmonic analysis indicates a strong excitation of the first mode and a much lower excitation level of the second and third modes(Figure A4), similarly to the cases of varying stiffness (cf. Figure 4). The corresponding SPLvalues shown in Figure 11 reveal a simple dependence between the radiated sound and thematerial density: the heavier the wing, the lower is the noise level induced during theflapping. The largest contribution comes again from the first and third eigenmodes.

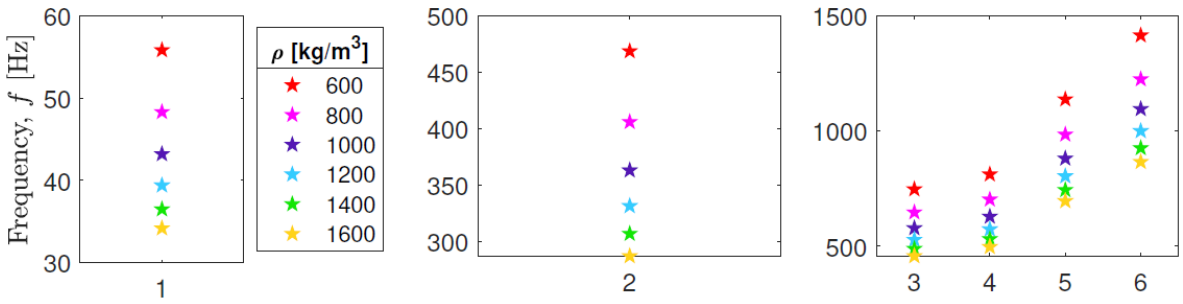


**Figure 10** Effect of density variation on modal frequencies of insect wing

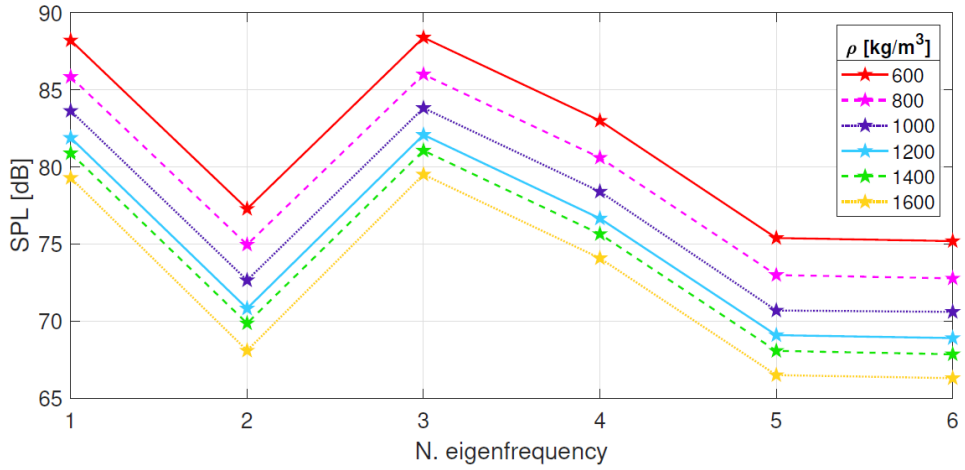


**Figure 11** Effect of density variation on the radiated noise by the wing

# 4 DISCUSSION AND TOWARDS METAMATERIAL-BASED ARTIFICIAL WING

The obtained results provide useful insights into the process of sound generation by structural motions of a flapping wing.

We observed the highest level of noise at the beginning of a flapping cycle that gradually decreases in time. Though the applied excitation matches the modal shape of the fundamental bending mode, the same level of sound is generated by the first flexural mode having a two-order lower amplitude. This suggests that the flexibility of the wing is crucial not only for its aerodynamics but also for the vibroacoustic properties.

We also found out that various parts of the wing generate different levels of noise. The strongest noise is radiated closer to the tip of the wing and propagates perpendicular to the wing surface in both directions.

Our analysis clarified that, different mechanical properties for the membranes and veins influence eigenfrequencies of the wing, but not the mode shapes and the efficiency of the mode excitation. Moreover, the radiated sound levels are also almost insensitive to the variations of the Young's modulus. In contrast, the increase of the mass density allows for reducing the SPL, but the weight of the wing becomes large which requires larger lift power and load-bearing capacity, and thus, is disadvantageous for applications.

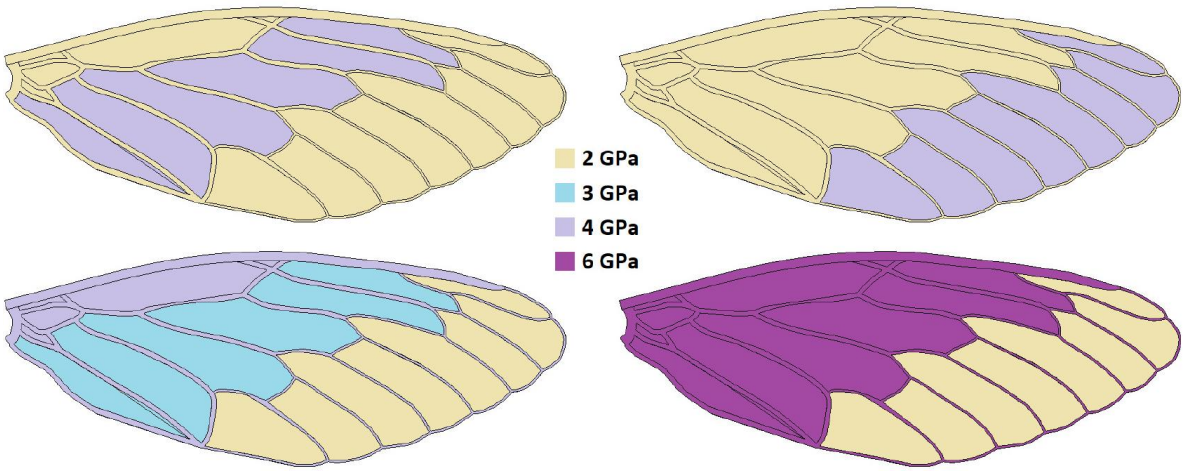


**Figure 12** The wing model with different Young's modulus areas

So far, we have analyzed simultaneous variations of the mechanical and material parameters for the whole wing. Yet, since the sound generation is nonuniform along the wing surface, it seems promising to control the noise radiation by applying the metamaterial principles, i.e., by introducing local variations of the parameters.

To verify this idea, we divided the wing into three areas and assigned to them different Young's modulus values as indicated in Figure 12. In the two cases (Figure 12 top), the veins are soft with $E_v$ = 2 GPa, while the membranes at the wing's tip are either soft, $E_m$ = 2 GPa, or stiff, $E_m$ = 4 GPa. The remaining two wing areas have either different (case 1) or identical stiffness (case 2). In the other two cases (Figure 12 bottom), the veins are stiff with $E_v$ = 4 GPa (case 3) or $E_v$ = 6 GPa (case 4), while themembranes are soft, $E_m$ = 2 GPa at the tip and stiff near the base with $E_m$ = 3 GPa and $E_m$ = 4 GPa, respectively.

To understand how the heterogeneous mechanical properties influence the wing's (aero-)dynamics, we calculated the eigenfrequencies (Figure 13) and the radiated SPL. (Figure 14).

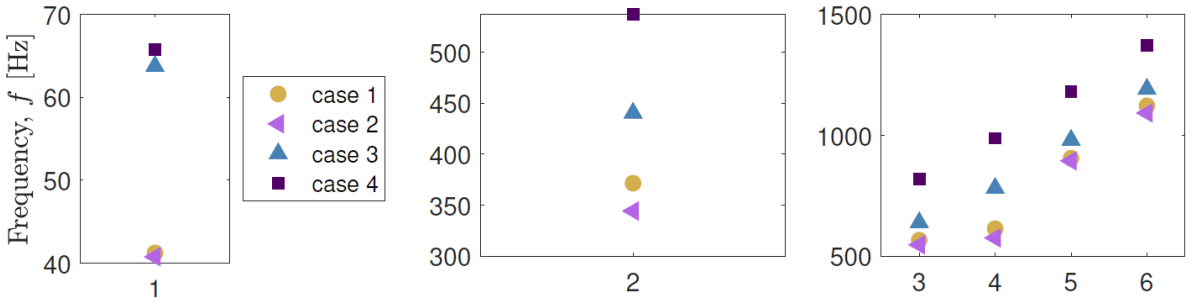


**Figure 13** Effect of density variation on modal frequencies of insect wing

The variations of the eigenfrequencies obey the same rules as derived above for the "homogeneous" wing (Figure 13 cf. Figure 2). Namely, softer wings have lower eigenfrequencies, and stiffer wings have larger eigenfrequencies. Note that since the overall stiffness of the wing in cases 1 and 2 is almost identical, the corresponding wing models have almost the same eigenfrequencies.

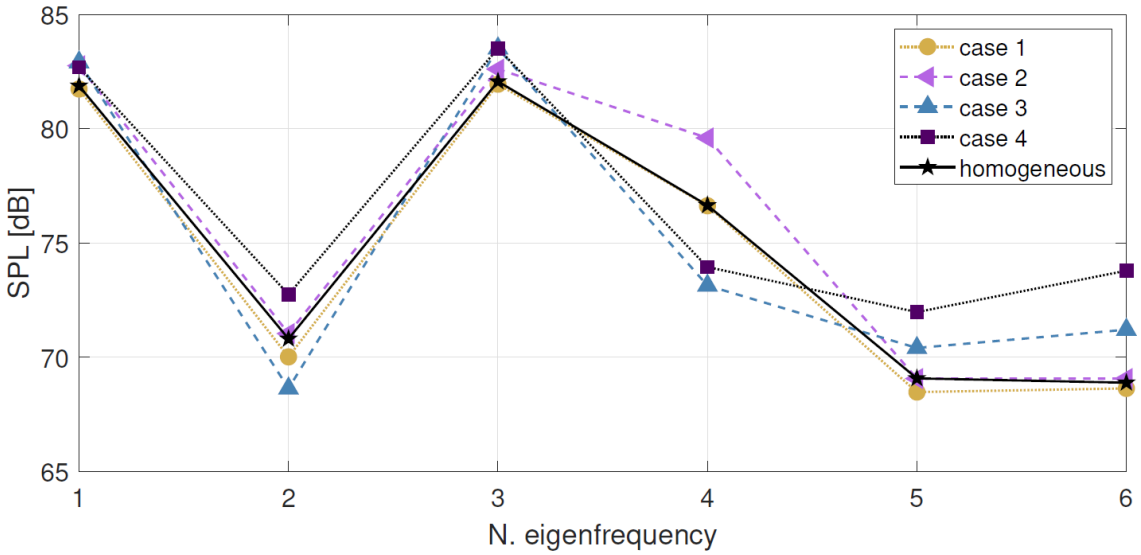


**Figure 14** Effect of gradient local variation of Young's modulus of wing on theradiated noise

The SPLs associated with each eigenfrequency in cases 1-4 undergo much larger variations as compared to those for the "homogeneous" wings (Figure 14 cf. solid lines in Figure 6). In particular, the differences for the first and third eigenmodes reach 2 dB, while for the fourth mode, they are around 7 dB. Despite comparatively small absolute values, even 1 dB noise reduction is considered as a big gain in vibroacoustic problems[32]. Therefore, we conclude that local variations of mechanical (and material) properties can be used to control sound radiated by structural motions of an artificial wing and are promising to develop low-noise artificial flapping wings.

Note that the results reported in Figure 14 demonstrate the possibility of noise control by tailoring the mechanical properties of different parts of the wing but give no guidelines on how to minimize generated noise. The latter is a complex problem that requires a systematic study of how local variations in the wing's morphology beneficial for noise reduction influence the overall aerodynamics of the wing, including the flight efficiency, power consumption, and the balance between rigidity and flexibility. This analysis should be performed separately by applying proper optimization techniques, e.g., as proposed in Refs.[33,34,35,36], and is, thus, out of the scope of the present work.

# 5 CONCLUSION AND OUTLOOK

This work numerically studied the structural and vibroacoustic characteristics of a flapping artificial insect wing with different mechanical and material properties. The obtained results provided insights into sound radiation conditions by oscillating wings and demonstrated how local modifications of the properties of various wing areas can be used to manipulate the level of radiated noise.

The latter idea has recently been applied to enhance control over acoustic waves in randomly structured metamaterials[37]. For bio-inspired applications, it opens new horizons for sound control in artificial wings. We envision several possible research directions, e.g., the application of topology optimization techniques to minimize noise radiation[38], the implementation of non-smooth pre-stretched membranes with large surface viscosity to reduce generated noise, or the modification of the wing morphology by introducing locally resonant response, which is, surprisingly, naturally present in real insect wings[39]. These studies require a comprehensive analysis of the complex interrelated aerodynamic, mechanical, and vibroacoustic characteristics to achieve a required functionality of a wing. Once performed, they will deliver fruitful results for further developments in robotic devices with flexible flapping wings.

# 6 APPENDIX A. SIMULATION DETAILS AND SUPPLEMENTARY RESULTS

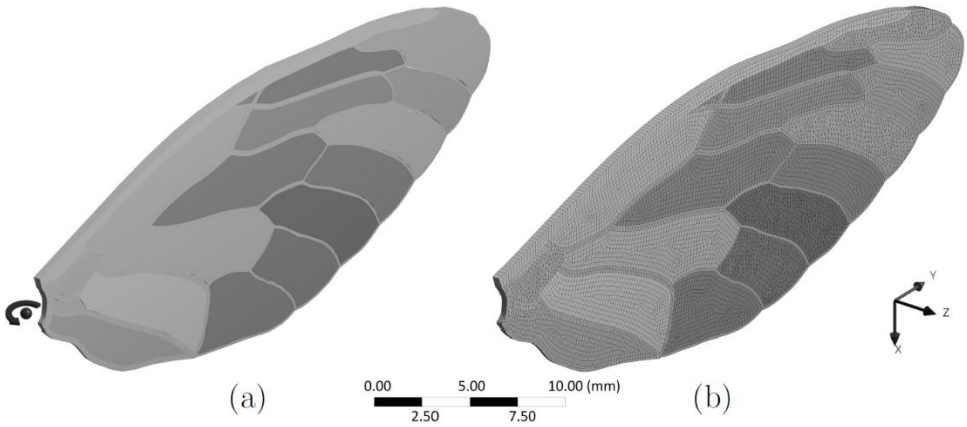


**Figure A1** (a) Center of rotation (root of the wing) (b) the finite-element mesh of the wing model. Different gray colors are used to highlight the wing structure.

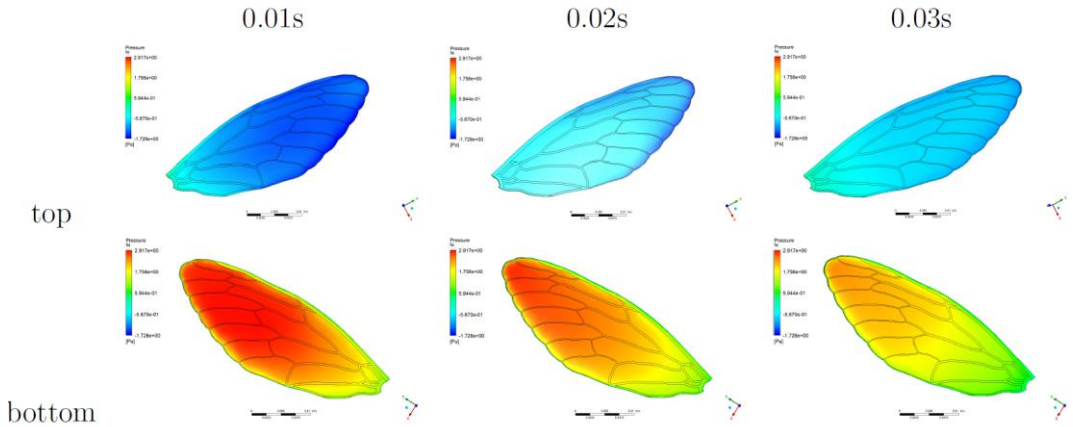


**Figure A2** Pressure areas on the bioinspired model $E_v$ = 6 GPa, $E_m$ = 1.5 GPa.

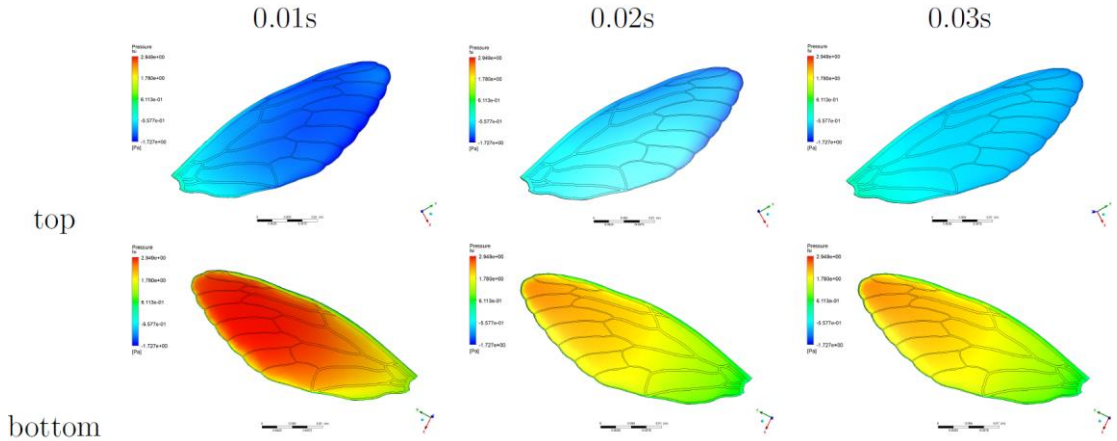


**Figure A3** Pressure areas on the bioinspired model $E_v$ = 6 GPa, $E_m$ = 2 GPa.

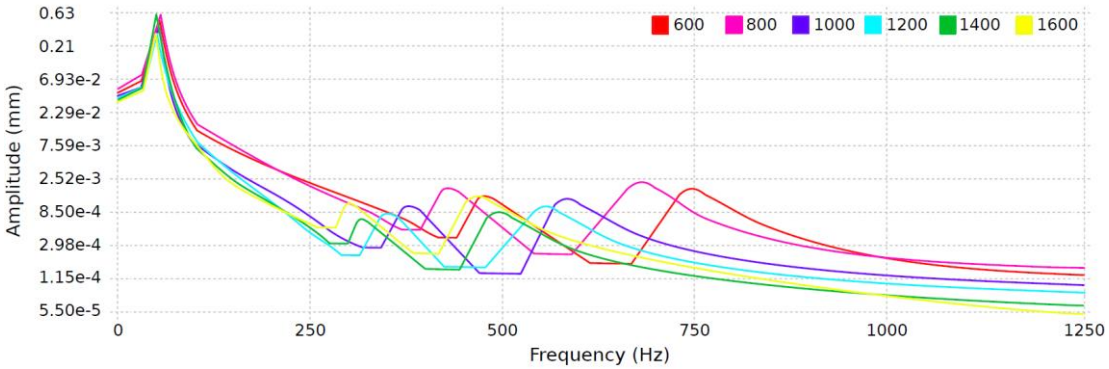


**Figure A4** Effect of density variation on FRF of the wing, $E_v$ = 2 GPa, $E_m$ = 2 GPa.

# 7 REFERENCES


1. P. Fratzl and R. Weinkamer. Nature's hierarchical materials. *Prog. Mater. Sci.*, 52:1263–1334,2007.
2. J. Vincent. *Structural biomaterials*. Princeton University Press, Princeton and Oxford, 2012.
3. J. U. Surjadi, L. Gao, H. Du, X. Li, X. Xiong, N.X. Fang, and Y. Lu. Mechanical metamaterialsand their engineering applications. *Adv. Engng. Mat.*, 21:1800864, 2019.
4. T.A. Schaedler, A. J. Jacobsen, A. Torrents, A. E. Sorensen, J. Lian, J. R. Greer, L. Valdevit, and W. B. Carter. Ultralight metallic microlattices. Science, 334:962–965, 2011
5. X. Zheng, H. Lee, T. H. Weisgraber, M. Shusteff, J. DeOtte, E. B. Duoss, J. D. Kuntz, M. M. Biener, Q. Ge, J. A. Jackson, S. O. Kucheyev, N. X. Fang, and C. M. Spadaccini. Ultralight, ultrastiff mechanical metamaterials. Science, 344:1373–1377, 2014.
6. G. W. Milton and A. V. Cherkaev. Which elasticity tensors are realizable? J. Eng. Mater. Technol., 117:483–493, 1995.
7. L. R. Meza, S. Das, and J. R. Greer. Strong, lightweight, and recoverable three-dimensional ceramic nanolattices. Science, 345:1322–1326, 2014.
8. M. Miniaci, A. O. Krushynska, A.S. Gliozzi, N. Kherraz, F. Bosia, and N. M. Pugno. Design and fabrication of bioinspired hierarchical dissipative elastic metamaterials. Phys. Rev. Appl., 10:024012, 2018.
9. A. O. Krushynska, M. Miniaci, F. Bosia, and N. M. Pugno. Spider web-structured labyrinthine acoustic metamaterials for low-frequency sound control. New J. Phys., 19:105001, 2017.
10. A. B. Kesel, U. Philippi, and W. Nachtigall. Biomechanical aspects of the insect wing: an analysis using the finite element method. Comput. Biol. Med., 28:423–437, 1998.
11. C. P. Ellington, C. van den Berg, A. P. Willmott, and A. L. R. Thomas. Leading-edge vortices in insect flight. Nature, 384:626–630, 1996.
12. S. A. Combes and T. L. Daniel. Flexural stiffness in insect wings ii. spatial distribution and dynamic wing bending. J. Exp. Biol., 206:2989–2997, 2003.
13. J. Sun and B. Bhushan. The structure and mechanical properties of dragonfly wings and their role on flyability. Comptes Rendus M´ecanique, 340:3–17, 2012.
14. N.S. Ha, Q.T. Truong, N.S. Goo, and H. C. Park. Relationship between wingbeat frequency and resonant frequency of the wing in insects. Bioinspir. Biomim., 8:046008, 2013.
15. I. Zhilyaev, D. Krushinsky, M. Ranjbar, A. O. Krushynska, "Hybrid machine-learning and finite-element design for flexible metamaterial wings", Materials and Design, 2022.
16. A. O. Krushynska, I. Zhilyaev, N. Anerao, M. Ranjbar, M. C. Yilmaz, M. Murat, "3D-Printed Flexible Wings with Metamaterial Functionalities", 15th International Congress on Artificial Materials for Novel Wave Phenomena – Metamaterials 2021, ave Phenomena – Metamaterials 2021, New York, USA, Aug. 2nd –7th, 2021.
17. R. J. Wootton, R. C. Herbert, P. G. Young, and K. E. Evans. Approaches to the structural modelling of insect wings. Phil. Trans. R. Soc. Lond. B, 358:1577–1587, 2003.

18. M. Hamamoto, Y. Ohta, K. Hara, and T. Hisada. Application of fluid structure interaction analysis to flapping flight of insects with deformable wings. Adv. Robot., 21:1–21, 2007.
19. J. Young, S. M. Walker, R. J. Bomphrey, G. K. Taylor, and A. L. R. Thomas. Details of insect wing design and deformation enhance aerodynamic function and flight efficiency. Science, 325:1549– 1552, 2009.
20. A. Krushynska, I. Zhilyaev, D. Krushinsky, N. Anerao, M. C. Yilmaz, M. Ranjbar, “Metamaterial pattern enabling control over sound produced by flapping artificial wings”, Metamaterials, Photonic Crystals and Plasmonics | META 2022, Torremolinos, Spain, 19-22, July 2022.
21. H. Rajabi and S.N. Gorb. How do dragonfly wings work? a brief guide to functional roles of wing structural components. Int. J. Odonatol., 23:23–30, 2020.
22. T. Nakata and H. Liu. A fluid–structure interaction model of insect flight with flexible wings. J. Comp. Phys., 231:1822–1847, 2012.
23. C. J. Clark and E. A. Mistick. Humming hummingbirds, insect flight tones and a model of animal flight sound. J. Exp. Biol., 223:jeb214965, 2020.
24. K.V.R. Manikanta, N. Muralikrishna, N. Sathish, and G. Sampath Kumar. Case study on investigation of aerofoil for flapping wing aircraft. Int. J. Eng. Res. Tech., 4:19–25, 2015.
25. A. O. Krushynska, I. Zhilyaev, N. Anerao, M. Ranjbar, M. C. Yilmaz, M. Murat, “Additively manufactured metamaterial-based flexible wings for micro-robotic applications”, The 5th International Conference on Material Strength and Applied Mechanics (MSAM 2022), Qingdao, Shandong, China, April 15-18, 2022.
26. U. Oberd¨orster and P.R. Grant. Predator foolhardiness and morphological evolution in 17-year cicadas (magicicada spp.). Biol. J. Linn. Soc., 90:1–13, 2007.
27. J.-S. Chen, J.-Y. Chen, and Y.-F. Chou. On the natural frequencies and mode shapes of dragonfly wings. J. Sound Vib., 313:643–654, 2008.
28. I. Zhilyaev, N. Anerao, A.G.P. Kottapalli, M. C. Yilmaz, M. Murat, M. Ranjbar, A. O. Krushynska, “Fully-printed metamaterial-type flexible wings with controllable flight characteristics”, Bioinspiration & Biomimetics, 2021.
29. S.A. Wainwright, W.D. Biggs, J.D. Currey, and J.M. Gosline. Mechanical Design in Organisms. Princeton University Press, Princeton, New Jersey, 1982.
30. B. W. Young. Energy methods of structural analysis. The Maxmillan Press Ltd, London, 1981.
31. N.S. Ha, Q.V. Nguyen, N.S. Goo, and H.C. Park. Static and dynamic characteristics of an artificial wing mimicking an allomyrina dichotoma beetle’s hind wing for flapping-wing micro air vehicles.
32. S. Marburg. Developments in structural-acoustic optimization for passive noise control. Arch. Comp. Meth. Eng., 9:291-370, 2002.
33. M. Ranjbar, St. Marburg, and H.-J. Hardtke. Structural-acoustic optimization of a rectangular plate: A tabu search approach. Finite. Elem. Anal. Des., 50:142-146, 2012.
34. M. Ranjbar, L. Boldrin, F. Scarpa, S. Niels, and S. Patsias. Vibroacoustic optimization of anti-tetrachiral and auxetic hexagonal sandwich panels with gradient geometry. Smart Mater. Struct., 25:054012, 2016.
35. A. Hosseinkhani, D. Younesian, and M. Ranjbar. Vibro-acoustic analysis and topology optimization of anti-tetra chiral auxetic lattices driven by different colored noises. Int. J. Struct. Stab. Dyn., 20:2050113, 2020.
36. M. S. Mazloomi, M. Ranjbar, L. Boldrin, F. Scarpa, S. Patsias, and N. Ozada. Vibroacoustics of 2d gradient auxetic hexagonal honeycomb sandwich panels. Comp. Struct., 187:593-603, 2018.
37. L. D'Alessandro, A. O. Krushynska, R. Ardito, N. M. Pugno, and A. Corigliano. A design strategy to match the band gap of periodic and aperiodic metamaterials. Sci. Rep., 10:1-13, 2020.
38. A. Hosseinkhani, D. Younesian, M. Ranjbar, and F. Scarpa. Enhancement of the vibro-acoustic performance of anti-tetra-chiral auxetic sandwich panels using topologically optimized local resonators. Appl. Acoust., 177:107930, 2021.
39. T. R. Neil, Z. Shen, D. Robert, B. W. Drinkwater, and M. W. Holderied. Moth wings are acoustic metamaterials. Proc. Natl. Acad. Sci., 117:31134-31141, 2020.